JOURNAL OF MATERIALS SCIENCE 23 (1988) 4209–4216

Viscoelastic analysis of a polyurethane thermosetting resin under relaxation and at constant compression strain rate

Y. LETERRIER, C. G'SELL
Laboratoire de Physique du Solide (U.A. CNRS 155), Ecole Nationale Supérieure des Mines de Nancy, Parc de Saurupt, 54042 Nancy cedex, France

The evolution of the viscoelastic behaviour of a polyurethane resin was investigated on the basis of uniaxial compression tests in stress relaxation and at constant strain rate. Both methods were applied to PUR specimens whose curing cycle was interrupted at different steps. The experimental data were precisely modelled in terms of a three-parameter constitutive equation whose general form was derived from the Kohlrausch relaxation law. The viscoelastic behaviour was followed during the cross-linking process and during the final cooling ramp. A close correlation was found between the degree for cross-linking and the elastic modulus increase during the curing period. Furthermore, it was stated that the evolution of the viscoelastic parameters during the cooling phase describes in a quantitative way the construction of the glassy behaviour and that it controls the development of internal stresses in PUR mouldings.

1. Introduction

Thanks to the considerable flexibility of their formulation, polyurethane resins (PUR) are now applied to a very large variety of industrial uses including rigid or flexible foams, rigid or rubberlike plastics, fibres, adhesives and coatings [1–5]. The PUR thermosets are of particular importance due to a favourable combination of strength, chemical resistance and high optical properties. Furthermore, they can be readily processed by direct in-mould polymerization. In this technology, isocyanate monomers and alchohol oligomers are mixed together with a suitable catalyst, the final structure and properties depending not only on the nature of the basic chemicals, but also on the temperature schedule of the curing process [6]. It is, therefore, of great importance to characterize the polymer during the crosslinking cycle and after it is completed. Various methods have been proposed to analyse this evolution [7–12]. Spectroscopic methods (e.g. IRFT [13, 14]) are now widely applied for such an investigation since they indicate the degree of crosslinking in real time through the significant evolution of the isocyanate band. Nevertheless, they have some limitations. For example, they cannot be applied to opaquely filled resins. Also their interpretation becomes hazardous if two bands overlap. It is, therefore, essential to find reliable alternative methods to study the curing process.

Among the latter techniques, viscoelastic mechanical analysis is of considerable interest for the characterization of curing resins, and particularly for that concerning the evaluation of the internal stresses which may appear during the cooling of the polymer in the mould. However, although the viscoelastic analysis is now widespread for qualitative inspection of polymers, the precise determination of viscoelastic parameters requires rigorous experimental conditions. Furthermore, the physical modelling of the constitutive law thus obtained is still the object of an active debate.

The aim of this work is twofold.

(i) to corrrelate with a minimum number of parameters the viscoelastic data obtained from compression tests at a constant strain rate and stress relaxation tests, and,

(ii) to apply this modelling to the characterization of a typical polyurethane resin during the course of its curing process.

2. Experimental procedure and results

2.1. Material preparation

The PUR considered here is an industrial grade obtained from bulk polycondensation of an aliphatic diisocyanate and a polydispersed triol, with a tin dibutylaurate catalyst. The bulk synthesis was conducted in a closed reactor under agitation. Samples were obtained by pouring this prepolymer into a rubber tube, and the polymerization was then completed in a drying oven according to the heating cycle described in Fig. 1. Cylindrical specimens, 20 mm long and 6 mm diameter, were then readily obtained by cutting the tube and carefully grinding the ends. In a complementary study, the polymerization of the PUR was characterized by the following technique: a drop of the resin was squeezed between two KBr windows and introduced in the heating stage of an IRFT spectrometer. Material spectra were recorded while the curing cycle was conducted in order to determine the evolution of the degree of crosslinking. The results are displayed in Fig. 1 together with the temperature

0022–2461/88 $03.00 + .12

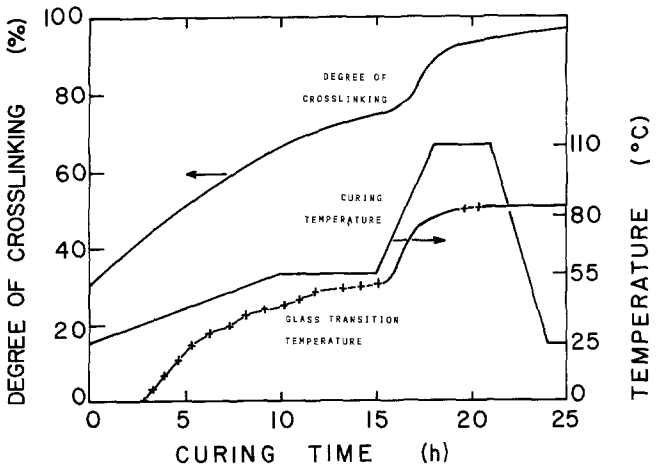

Figure 1 Temperature programme of the curing process, evolution of the degree of crosslinking and evolution of the glass transition temperature.

profile. They show that the gel point occurs during the second temperature rise between 15 and 18 h and that the cross-linking is almost completed at the end of the upper temperature plateau. The glass transition temperature (T_g) was also measured by DSC, at a temperature rate of 10° C min^{-1}. It is evident in Fig. 1 that T_g is always lower than the curing temperature, reaching 80° C at the end of the cycle. This value was confirmed by dynamic mechanical analysis performed with a Metravib viscoelasticimeter at 7.8 Hz.

2.2. Mechanical testing procedures

Uniaxial compression was chosen for the viscoelastic tests. This geometry was preferred to others because it requires samples of a limited size and simple cylindrical shape. It also offers an optimized transmission of stress [15–16]. Great care had been taken in machining and grinding the ends of the moulded cylinders so that smooth parallel surfaces and sharp clean edges could be obtained with a precision better than 25 μm following the prescription of the current standards (ASTM D 695).

The specimen dimensions provide a reasonable compromise between the conflicting needs to reduce buckling propensity by decreasing the length–section ratio, and to minimize the friction on the compression tools which increases with this ratio [17]. With the specimens employed here, buckling was encountered only for compression strains exceeding 10%, far above the investigated range. Also no significant barrelling was measurable in the experiments.

2.3. Experimental set-up

The special compression cell which was designed for this study is shown in Fig. 2. It provides a good axiality of the compression stress and a sharp measurement of the strain. The tools are made of two stems which are guided by precision linear ball bearings mounted in a stainless steel holder (a). The pressing heads (b) are perpendicular to the compression axis within 5 μm error. The lower stem (c) is fitted free on a ball pivot (d) on the load cell. The upper stem (e) is firmly attached to the crosshead of the Instron testing machine (f). The strain transducer (g) (Instron ref 2620-602) is clipped near the level of the pressing heads. the sample (h) is inserted between the pressing heads by means of tweezers. The above cell was mounted in an Instron screw-driven testing machine equipped with a strain servo control module. Fig. 3 shows the whole apparatus.

The testing temperature was controlled by means of an environmental chamber which was developed in the laboratory. This chamber has several novel aspects, the principal one being its very fast heating rate. Thanks to the two hot air turbines with copper thermic buffers, the desired specimen temperature (up to 200° C) can be reached and controlled within a time of about 300 sec, with an accuracy better than ± 0.2° C. This very short response time is of great interest for various applications, for example when mechanical experiments are performed with incompletely cured PUR as presented later. The temperature in the chamber was controlled and recorded by means of four thermocouples which are disposed as indicated

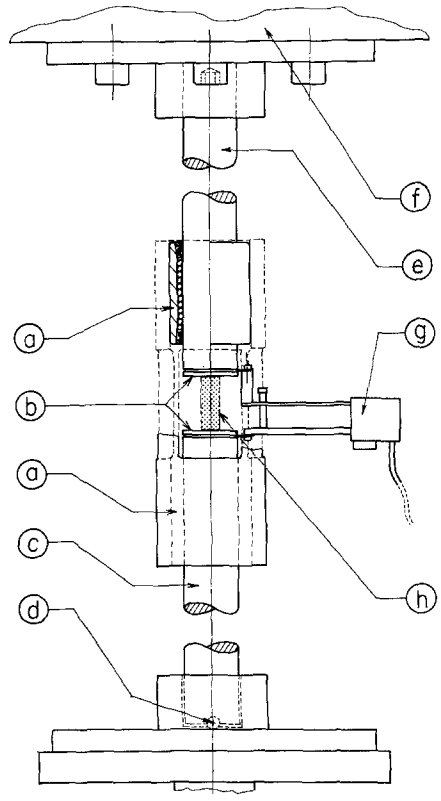

Figure 2 Detailed diagram of the compression cell (a, stainless steel holder, b, pressing heads, c, lower stem, d, ball pivot, e, upper stem, f, Instron machine crosshead, g, strain transducer, h, compression sample).

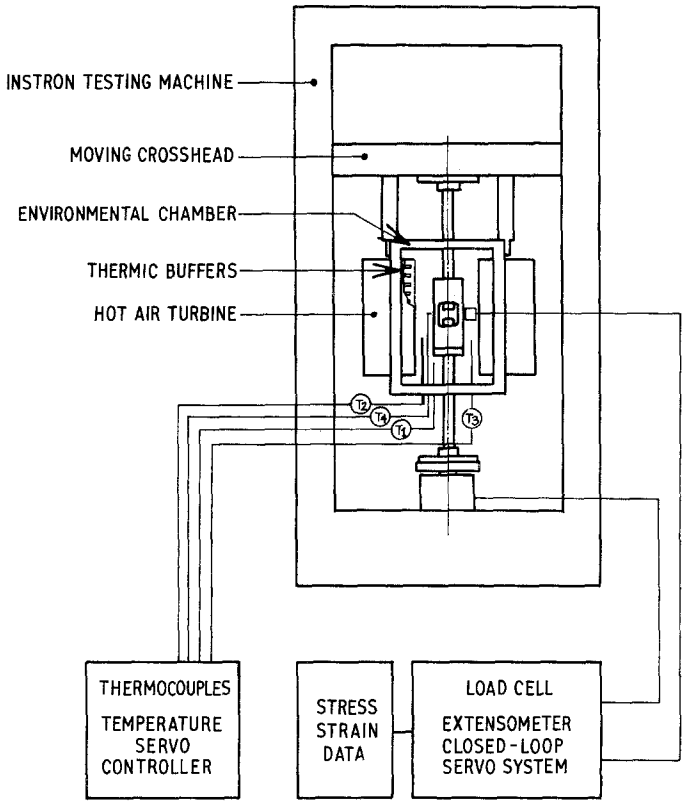

Figure 3 Overall experimental device.

in Fig. 3: T_1 is connected to the temperature servo controller, T_2 and T_3 give the temperature of the two turbines, and T_4 measures the specimen's local temperature. A temperature gradient less than 0.5° C was thus obtained in the chamber width.

The compression strain applied to the specimen was controlled through the closed loop servo system of the Instron machine. In this device, the regulated strain was the deflection of the compression extensometer and not the displacement of the crosshead of the testing machine (which includes the deformation of the machine). A careful check of the testing set up showed that, in standard conditions, the axiality defect was less than 1 μm, and the small force introduced by the extensometer did not exceed 10^{-4} of the force measured at room temperature.

In all the matter below, the compression strain will be defined as the relative reduction of length $\varepsilon = (L_0 - L)/L_0$, and the compression stress as the load per unit original cross section $\sigma = P/A_0$. The letters t and θ will represent time and temperature respectively.

2.4. Compression tests at constant strain rate

A first series of tests were driven to determine the Young modulus of the PUR at different stages of its polymerization. Mouldings were quenched to room temperature at various times during the curing cycle, compression specimens were then machined and kept in a deep freezer to stop their cross-linking until they were mechanically tested. Thanks to the fast heating rate of the environmental chamber they could be brought again at the same temperature they were quenched from, before a noticeable amount of extra cross-linking could develop.

Compression tests were then performed at a constant strain rate of $\dot{\varepsilon} = 1.667 \times 10^{-4}\,\text{sec}^{-1}$. The instantaneous Young modulus, E_0, was obtained from the initial slope of the $\sigma(\varepsilon)$ curve at $\varepsilon = 0$. Its evolution during the curing process is displayed in Fig. 4 together with the temperature profile. Several successive stages are seen. Before the gel point (0 to 15 h) the resin is in a nearly viscous state with a very weak elastic component. The small trough on the E_0 curve, between 15 and 16 h, is related to the temperature increase from 55 to 110° C; this fall of modulus is rapidly overcompensated by the cross-linking process, while the specimen develops a rubber-like behaviour and a gradual increase of E_0. The sample remains rubbery as long as the temperature, θ, is higher than the glass transition temperature, T_g. Nevertheless, it happens finally during the cooling ramp that θ becomes lower than T_g and the PUR becomes glassy with a three-decade increase of E_0, reaching almost 2800 MPa at the end of the cooling.

It appears from the above results that the cooling period is the more critical part of the curing cycle insofar as it corresponds to the emergence of the

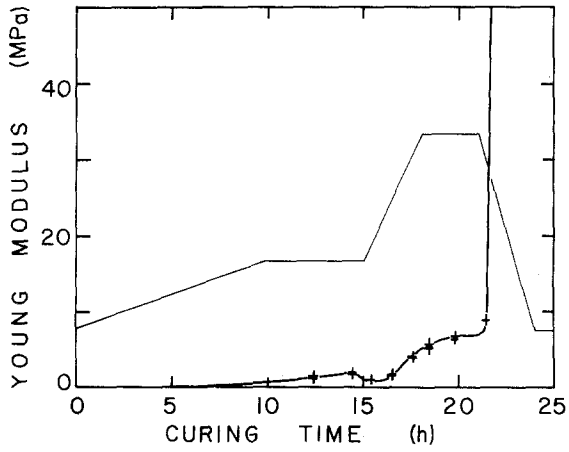

Figure 4 Young modulus evolution of the PUR during the curing process.

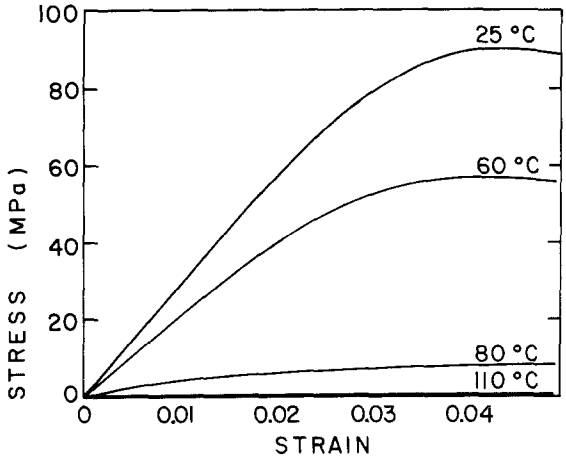

Figure 5 Experimental stress-strain curves obtained at constant strain rate 1.67×10^{-4} sec^{-1} at four temperatures.

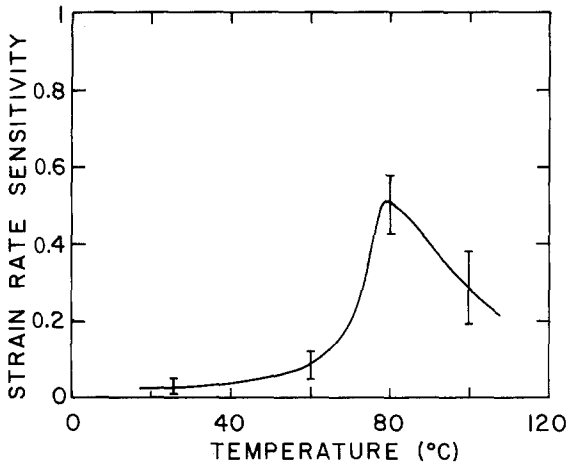

Figure 7 Temperature evolution of the strain rate sensitivity, m.

glassy state and to the possible construction of internal stresses. Consequently, particular attention was paid to the viscoelastic properties of the specimens sampled in the cooling ramp. For this detailed study, stress-strain properties were tested at various strain rates ranging from $\dot{\varepsilon} = 10^{-6}$ to 10^{-3} sec^{-1}, at seven temperatures from 110 to 25° C. Typical curves obtained in this way are shown in fig. 5. It is evident that the initial elastic response is relayed, for strains larger than 0.005, by a viscoelastic behaviour. Plastic yielding is finally observed at a strain of about 0.04.

Compression stress was also investigated as a function of strain rate. Typical curves at room temperature (Fig. 6) show the gradual increase of stress with $\dot{\varepsilon}$. The strain rate sensitivity coefficient is defined as $m = (\partial \ln \sigma / \partial \ln \dot{\varepsilon})_{\varepsilon}$. It was found to be very sensitive to temperature showing a definite peak in the vicinity of T_g (Fig. 7).

Although the compression tests at constant strain rate are of convenient use for the determination of the Young modulus and for the characterization of the yield process, their accuracy is limited for the determination of the viscoelastic behaviour which is correlated to the curvature of the $\sigma(\varepsilon)$ curve. As one can note in Figs 5 and 6, this curvature is quite tiny at small strains. It increases as ε grows but the interpretation of the behaviour becomes more and more questionable as the contribution of the preplastic deformation increases. It will be shown in the following section that stress relaxation tests are preferable for the precise assessment of the viscoelastic behaviour with better accuracy.

2.5. Stress relaxation

Stress relaxation tests were performed according to the following procedure. The specimen was brought to the fixed initial strain $\varepsilon_0 = 10^{-3}$, 5×10^{-3}, 10^{-2}, 3×10^{-2}, with a fast loading rate of 10^{-2} sec^{-1}. The strain was then maintained at this value by means of the closed loop servo control system. The stress evolution $\sigma(t)$ was recorded as a function of time for a relaxation period of 10 000 sec, the temperature being controlled in the meanwhile with a precision better than ± 0.2° C. Several relaxation curves are displayed in Fig. 8 which represent the typical viscoelastic behaviour of the material reheated to the same temperature from which they were quenched during the final cooling ramp of the curing cycle, that is at 75, 50, 35 and 25° C respectively. The initial value of the stress (at $t = 0$) corresponds to the elastic response of the PUR since it can be supposed that no relaxation processes are efficient during the very short straining time (1 sec for $\varepsilon_0 = 0.01$). The gradual decrease of σ during the relxation phase is associated with the

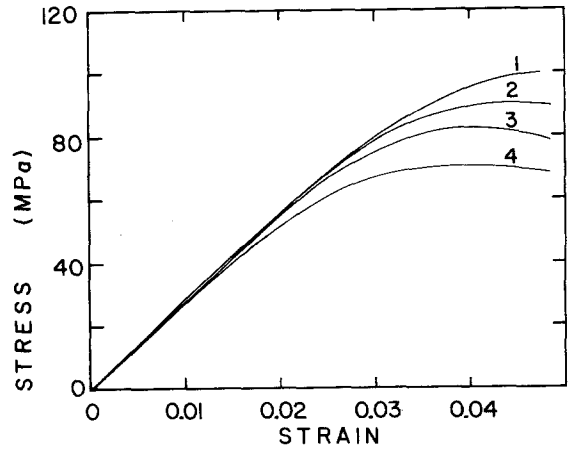

Figure 6 Experimental stress-strain curves obtained at room temperature (25° C), at four strain rates (1) 1.67×10^{-3} sec^{-1}, (2) 1.67×10^{-4} sec^{-1}, (3) 8.33×10^{-5} sec^{-1}, (4) 1.67×10^{-6} sec^{-1}.

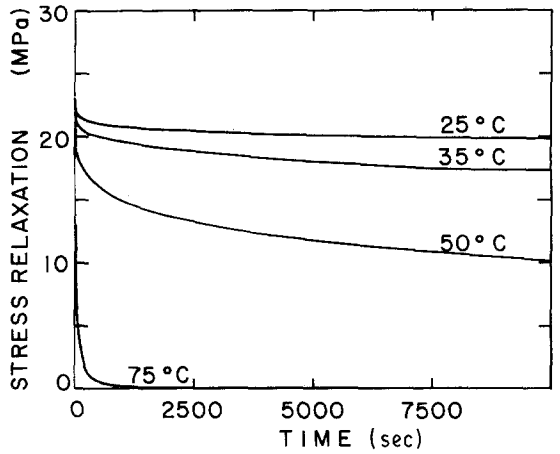

Figure 8 Experimental relaxation curves obtained at four temperatures. $\varepsilon_0 = 0.01$.

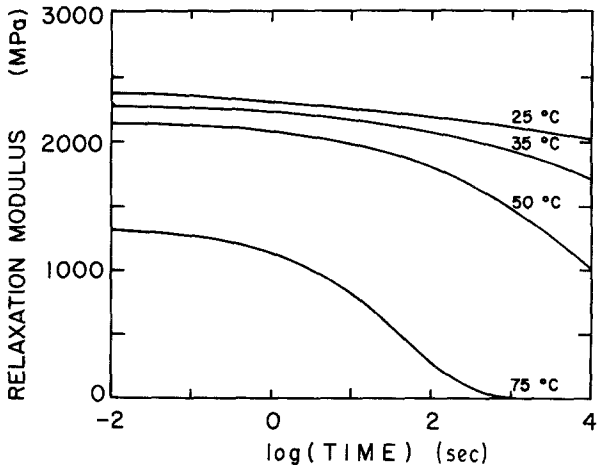

Figure 9 Relaxation modulus plotted against logarithm of time, calculated from the data of Fig. 8.

activation of viscoelastic conformational changes in the network structure. The relaxation rate is seen to become much slower as the testing temperature is reduced.

Following previous studies [18], these results were expressed in terms of the relaxation modulus $E(t) = \sigma(t)/\varepsilon_0$. It was found that, for a given time, the relaxation stress was proportional to the applied strain within an error of about 1%. Consequently, the viscoelastic behaviour of the PUR can be considered as "linear" and the relaxation modulus is therefore independent of strain. The decay of the modulus during the tests of Fig. 8 is represented in Fig. 9, with a logarithmic time scale which is more suitable for the evaluation of the material behaviour at both very short and very long times.

By comparison to tests at constant strain rate, stress relaxation tests are more sensitive to the viscoelastic response. This is because, in this test, there is a gradual decrease of the elastic component of strain as the viscoelastic component grows. In other words, the large elastic modulus of the material serves as an amplifier to the detection of viscoelasticity. Furthermore, since the total applied strain is very small, no significant plastic processes can disturb the investigation.

3. Analytic modelling of the viscoelastic behaviour

3.1. Stress relaxation behaviour

Among the very large number of mechanical models which were presented to describe the relaxation behaviour of polymers, the most classical one is based on a parallel combination of Maxwell elements, the so-called Maxwell–Wierchert model [18, 19]. the elementary relaxation response of the ith element is given by

$$E_i(t) = E_{0i} \exp(-t/\tau_i) \quad (1)$$

where E_{0i} is the original modulus at $t = 0$ associated to the element i and τ_i the characteristic relaxation time for this element. The resulting behaviour of a given polymer is then described by a particular distribution of N relaxation times, according to the following relation

$$E(t) = \sum_{i=1}^{N} E_{0i} \exp(-t/\tau_i) \quad (2)$$

or, for large N, by the relaxation spectrum $\Psi(\tau)$ through the equation

$$E(t) = \int_0^\infty \Psi(\tau) \exp(-t/\tau)\, d\tau \quad (3)$$

Various molecular models were largely developed to correlate the above formulations with microstructural parameters [20–22]. Among them it is worth noting the bead and spring model of Rouse [23] and Zimm [24] which was originally developed for dilute solutions. Specific molecular processes were invoked to interpret, for a variety of polymers, the particular shape of the relaxation spectrum [25, 26].

Alternatively, it has been found by Kohlrausch [27] that a continuous series such as Equation 3 may be approximated by an extended exponential law according to the following equation [27, 28]

$$E(t) = E_0 \exp[-(t/\tau)^n] \quad (4)$$

Here, the parameter n characterizes in a simplified way the distribution of the relaxation times. The case when n equals 1 corresponds to a single relaxation time (Maxwell model). The smaller n, the wider the range of active relaxation times. The characteristic time, τ, represents the time required for the initial modulus E_0 to be reduced by a factor of 1/e. The above approach was chosen in this study because of its great simplicity as a function of integral representations such as Equation 3, the total viscoelastic response being described by means of three parameters only. Moreover, the Kohlrausch law has been recently established on microstructural bases by Perez [29]. This author has shown that the non-elastic deformation of glassy materials can be analysed in terms of the correlated motion of strained microdomains. According to his analysis, anelastic processes result from the first kind of activation, corresponding to a cooperative

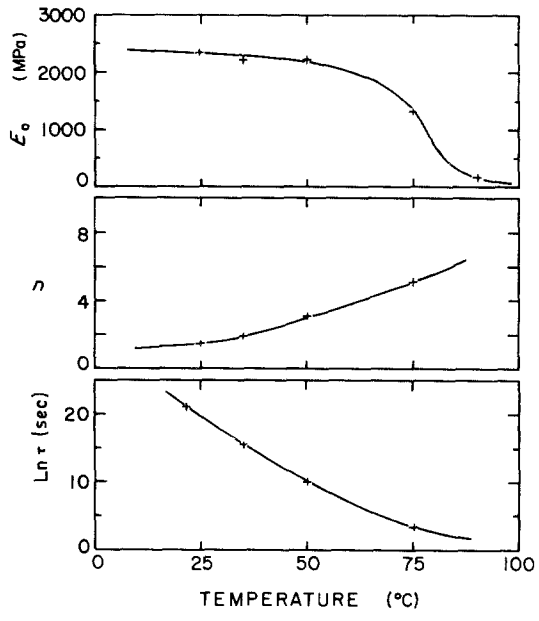

Figure 10 Temperature dependence of the Kohlrausch law parameters E_0, n and τ.

motion of defects areas. At this time, the deformation is reversible. If the elastic matrix reacts, a second activation appears. When both activation processes are correlated, plasticity is released. Perez has demonstrated that the relaxation equation obtained from this model leads with the Kohlrausch formalism.

In order to apply the above modelling to the experimental relaxation curves obtained in this work, the parameters E_0, n and τ were determined by the following procedure. In a first step, the elastic modulus E_0 was directly obtained from the initial stress at $t = 0$. In a second step, the two parameters n and τ were adjusted with a kind of multidimensional conjugate gradient method [30, 31]. In this computer method, the mean square difference between the experimental and the theoretical curves is considered as a mathematical surface whose minimum is searched by an optimized sequence of n and τ increments, following a "steepest descent" scheme. The best fitted values obtained for the PUR relaxed at different temperatures are displayed in Fig. 10.

3.2. Viscoelastic behaviour at constant strain rate

Since the Kohlrausch equation appears to be a simple and efficient representation of the viscoelastic response of the PUR during a relaxation test, it is of interest to derive its equivalent form for the case of a compression test at constant strain rate. The basic link between the two types of testing is that, for a constant strain rate test, the slope of the stress–strain curve at any subsequent time of the constant strain rate period is equal to the relaxation modulus [19]. This property is based on the Boltzmann superposition principle which is written in its general form

$$\sigma(t) = \int_{-\infty}^{t} \frac{d\varepsilon(u)}{du} E(t-u)\, du \qquad (5)$$

In the case of the relaxation test, it reduces to the simple relaxation decay $\sigma(t) = \varepsilon_0 . E(t)$. for the test at constant strain rate, the polymer is supposed to be totally relaxed when the compression rate $\dot{\varepsilon}$ is applied at time $t = 0$, so that the Boltzmann equation becomes

$$\sigma(t) = \dot{\varepsilon} \int_{0}^{t} E(t-u)\, du \qquad (6)$$

This equation is readily differentiated to obtain the slope of the stress–strain curve at any strain $\varepsilon = \dot{\varepsilon} t$

$$\left[\frac{d\sigma}{d\varepsilon}\right]_{\varepsilon} = \frac{1}{\dot{\varepsilon}}\left[\frac{d\sigma}{dt}\right]_{t} = E(t) \qquad (7)$$

Introducing the Kohlrausch Equation 4 gives

$$\sigma(t) = \dot{\varepsilon} E_0 \int_{0}^{t} \exp\left[-(x/\tau)^n\right] dx \qquad (8)$$

With a change of variable, the integral 8 can be calculated

$$y = (x/\tau)^n \quad \text{thus } x = \tau y^{1/n}$$

and

$$dx = (\tau/n)\, y^{1/n-1} \qquad (9)$$

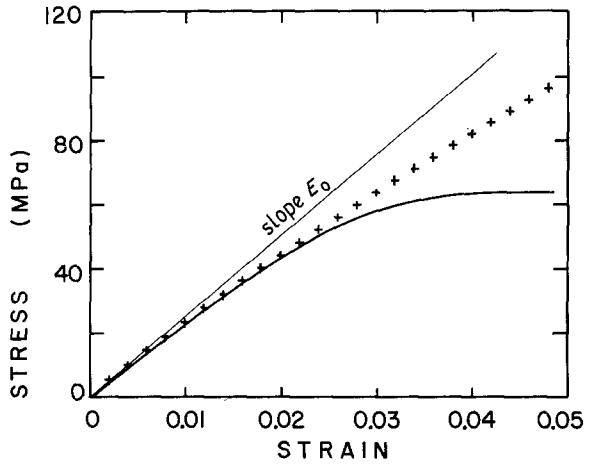

Figure 11 Comparison between an experimental stress–strain curve obtained at 50° C (continous) and the modelled curve (crosses).

This give the integral equation

$$\sigma(t) = \dot{\varepsilon} E_0 \tau/n \int_{0}^{(t/\tau)^n} \exp(-y)\, y^{1/n-1}\, dy \qquad (10)$$

Whose solution is given by the incomplete Euler function γ

$$\sigma(t) = (\dot{\varepsilon} E_0 \tau/n)\ \gamma\{(1/n;\ (t/\tau)^n\}. \qquad (11)$$

It should be noted that γ is defined for integer values of $1/n$ only. This is not a drastic limitation to the present purpose with regards to the wide range of the experimental values of $1/n$ (Fig. 10). In terms of the conventional stress and strain variables, Equation 11 is rewritten as

$$\sigma(\varepsilon, \dot{\varepsilon}) = (\dot{\varepsilon} E_0 \tau/n)\, \gamma\{1/n;\ (\varepsilon/\dot{\varepsilon}\tau)^n\} \qquad (12)$$

which is the constitutive equation of the viscoelastic material with the same three parameters E_0, n and τ as in Equation 4.

For numerical processing, analytic forms of Equation 12 are preferred. Two equivalent equations were derived, as indicated below

$$\sigma(\varepsilon, \dot{\varepsilon}) = (\dot{\varepsilon} E_0 \tau/n)\left(\sum_{k=0}^{\infty} (-1)^k \frac{(\varepsilon/\dot{\varepsilon}\tau)^{n(1/n+k)}}{k!\,(1/n+k)}\right) \qquad (13)$$

$$\sigma(\varepsilon, \dot{\varepsilon}) = \left(\dot{\varepsilon} E_0 \tau \frac{(1/n-1)!}{n}\right)\left[1 - (\exp\{-(\varepsilon/\dot{\varepsilon}\tau)^n\}) \times \left(\sum_{j=0}^{1/n-1} \frac{1}{k!} (\varepsilon/\dot{\varepsilon}\tau)^{nk}\right)\right] \qquad (14)$$

The latter equation is transformed using the limited development of an exponential to give

$$\sigma(\varepsilon, \dot{\varepsilon}) = \left(\dot{\varepsilon} E_0 \tau \frac{(1/n-1)!}{n}\right) \sum_{i=1/n}^{\infty} (-1)^i \times \left(\sum_{j=0}^{1/n-1} \frac{(-1)^j}{j!\,(i-j)!}\right) (\varepsilon/\dot{\varepsilon}\tau)^{ni} \qquad (15)$$

This form was finally adopted for practical data processing. The infinite series was found to converge very rapidly and thus could be limited to its first 20 terms.

Fig. 11 shows the validity of this analysis, by comparing an experimental stress–strain curve obtained at 50° C and the modelled curve, obtained from the corresponding values of the relaxation parameters E_0, n and τ given in Fig. 10. It is evident that the fit is good

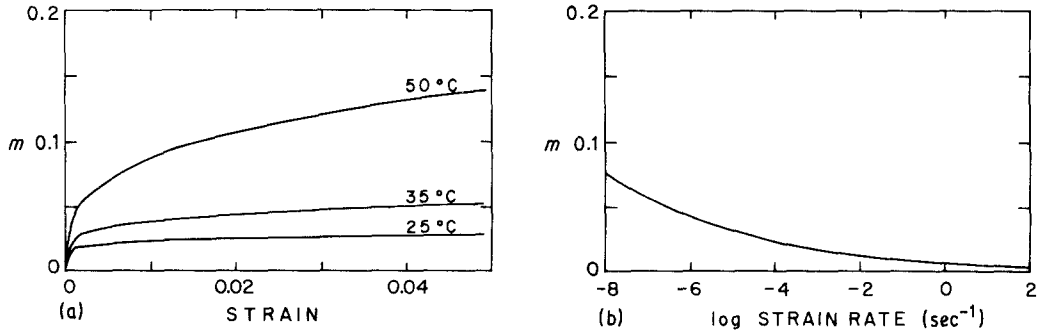

Figure 12 Evolution of the strain rate sensitivity, m (a) with strain, $\dot{\varepsilon} = 10^{-4}\,\text{sec}^{-1}$, (b) with strain rate, $\theta = 25°\text{C}$, $\varepsilon = 0.01$.

up to 2% of strain. Above that limit, the polymer response is affected by the supplementary contribution of the preplastic deformation mechanisms. According to the classical scheme, the total strain can then be decomposed as

$$\varepsilon = \varepsilon_{el} + \varepsilon_{visco} + \varepsilon_{pl} \qquad (16)$$

where the three terms represent the elastic, viscoelastic and plastic contributions. The interpretation of the plastic mechanisms is irrelevant to the present investigation and has been examined in some detail in other papers [29, 32]. The main interest of the present work is to give a quantitative method for determining the strain above which these plastic events begin to influence significantly the overall response of the material during testing at constant strain rate.

Another potential of the above treatment is to allow the analytic determination of the strain rate sensitivity coefficient $m = (\partial \ln \sigma / \partial \ln \dot{\varepsilon})_{\varepsilon}$. This coefficient is obtained by direct derivation of the constitutive equation $\sigma(\varepsilon, \dot{\varepsilon})$. It can be seen from Fig. 12 that m is not a fixed material parameter in the viscoelastic stage since it undergoes considerable variations both with strain and strain rate.

4. Potential applications of the compression viscoelastic analysis for PUR resins

It was demonstrated, in the preceding section, that the viscoelastic behaviour of PUR resins can be conveniently determined by the complementary use of compression testing in relaxation and at constant strain rate. Thanks to the reliability of the constitutive equation thus obtained, the experimental procedure can be applied to industrial purpose and in particular (i) to the routine evaluation of the curing process and, (ii) to the computation of the internal stresses which develop in the resin during specific moulding operations.

The first point has been illustrated in the paper by the evolution of the viscoelastic parameters E_0, n and τ during the course of the curing process of the thermosetting resin (Figs 4 and 10), the n and τ parameters being measurable below the glass transition temperature. The authors have also found, in another part of the work, that these parameters are very sensitive either to the chemical composition of the PUR, or to the temperature schedule of curing process. For example, in this second aspect, it was found that a 1 h increase of the 110° C plateau leads to the following modifications of the final viscoelastic parameters at room temperature: no change of E_0, 3% increase of n and 15% decrease of τ. It is evident that the E_0, n, τ triplet constitutes a valuable indicator of the microstructural state of the polymeric network.

The second application of the constitutive equation is concerned with the determination of residual stresses in moulded resin parts. These stresses arise from the inhomogeneous thermal contraction of the material during the cooling period. They are amplified by the gradual construction of the elastic modulus, and partly relaxed by viscoelastic flow [33]. The major problem in the calculation of fabrication stresses in a curing process is to take into account the temperature-dependent relaxation of the polymer. Some authors [6, 34–35] have developed various methods to predict these stresses in cured thermosetting resins. Their analyses are often based on a purely elastic modelling [36–38]. Furthermore the detailed evolution of the elastic modulus with temperature is often ignored, as if the material were instantaneously "frozen" from above T_g to room temperature [39]. Improved models including viscoelastic behaviour have been proved to be superior for the accurate evaluation of the internal stresses during and after cooling of the moulding [40, 41]. For such computations, the decreasing temperature ramp is discretized in individual steps $\Delta\theta$, each being followed by an incremental time Δt, as shown on Fig. 13. Each elementary temperature drop increases the internal stresses, while the waiting period lets the stresses relax to some extent. A simplified constitutive law like the Kohlrausch equation is then very convenient for the quantitative stress

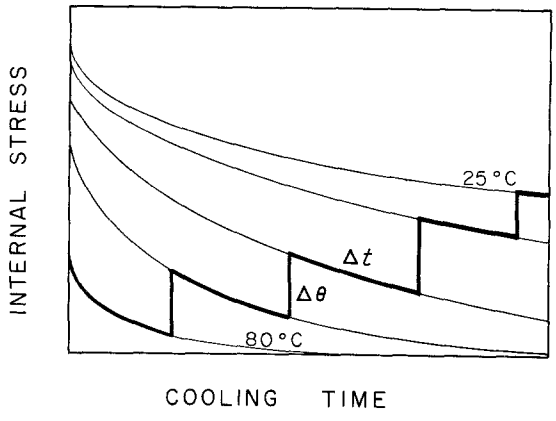

Figure 13 Time and temperature evolution of internal stress during the cooling ramp of the curing process described by an incremental formulation (schematic).

computation, its three parameters being determined at each temperature by a suitable interpolation of the experimental data, such as those shown in Fig. 10.

Last, the modelling of the fabrication stresses will allow the optimization of the cooling ramp profile. It should be noticed that the viscoelastic processes are more active at high temperatures while the increase of the elastic modulus is steeper at lower temperatures, A finely designed non-linear cooling schedule will help decreasing both the total cooling time and final internal stresses with respect to a standard linear ramp.

5. Conclusions

The viscoelastic behaviour of a thermosetting polyurethane was investigated by means of compression tests in stress relaxation and at constant strain rate. For this work, a novel compression cell was developed together with a fast-heating environmental chamber. The PUR specimens were tested at different steps during the curing process and, more particularly, during the final cooling ramp. The experimental data were processed in terms of a Kohlrausch relaxation equation, or of the corresponding stress–strain–strain rate constitutive law which was derived analytically.

The following were found

(1) The compression tests in stress relaxation and at constant strain rate are two complementary approaches to the viscoelastic behaviour of PUR resins since they provide separate information on the different components of strain; elastic, viscoelastic and plastic.

(2) The constitutive equation of the resin can be determined with a good precision by a set of three adjustable parameters, up to the initiation of plastic flow.

(3) The gradual cross-linking of PUR thermosets during the curing process is correctly monitored by the construction of the instantaneous elastic modulus, allowing the optimization of the curing schedule.

(4) The final viscoelastic parameters of the resin are very sensitive either to its composition or to the temperature profile of the curing process so that compression testing can serve as a good reliable production control method.

(5) The detailed evolution of the three viscoelastic parameters during the final cooling ramp controls the development of internal stresses in PUR parts fabricated by in-mould polymerization.

Acknowledgements

The authors are indebted to Professor C. Wippler and Dr M. Aboulfarraj of the E.A.H.P. (Institut Charles Sadron, Strasbourg) for performing the IRFT experiments.

References

1. J. A. BRYDSON, "Plastic Materials", Butterworth Scientific, Lond (1982).
2. D. L. QUESTAD, *Ind. Eng. Chem. Prod. Res. Dev.* **22** (1983) 138.
3. J. BLACKWELL and J. R. QUAY, *J. Polym. Sci.* **22** (1984) 1247.
4. J. P. TROTIGNON, M. PIPERAUD, J. VERDU and A. DOBRACZYNSK, "Précis de Matiéres Plastiques", Afnor-Nathan, Paris (1986).
5. D. C. MILES and J. H. BRISTON, "Technologie des Polymères", Dunod, Paris (1968).
6. J. DELMONTE, "Technology of Carbon and Graphite Fiber Composites", Van Nostrand Reinhold, New York (1981).
7. "Methods of Testing Plastics", British Standards Institution (1970) BS 2782.
8. HARRAH and A. LAUDOUARD, *Rheol. Acta* **24** (1985) 596.
9. J. M. DEALY, "Rheometers for Molten Plastics", Van Nostrand Reinhold, New York (1982).
10. P. J. HEINLE and M. A. ROGERS, *SPE J.* **25** (1969).
11. R. P. WHITE, Jr., *Polym. Eng. Sci.* **14** (1974) 50.
12. E. B. RICHTER and C. W. MACOSKO, *ibid.* **20** (1980) 921.
13. L. BUCKLEY and D. ROYLANCE, *ibid.* **22** (1982) 166.
14. C. W. MACOSKO and D. R. MILLER, *Macromol.* **9** (1976) 199.
15. R. A. FAVA, "Methods of Experimental Physics", Vol. 16. Part C Academic Press, New York (1980).
16. R. P. BROWN and F. N. B. BENNET, *Polym. Testing* **2** (1981) 125.
17. C. BORD, R. GIALLONARDO, P. A. SPORLI and G. VERCHERY, "Guide des Matières Plastiques en Mécanique", Cetim-Batelle, Senlis (1976).
18. J. D. FERRY, "Viscoelastic Properties of Polymers", John Wiley and Sons, New York (1970).
19. J. J. AKLONIS and W. J. MACKNIGHT, "Introduction to Polymer Viscoelasticity", John Wiley and Sons, New York (1983).
20. C. D. HAN, "Rheology in Polymer Processing", Academic Press, New York (1976).
21. K. WALTERS, "Rheometry", Chapman and Hall, London (1975).
22. J. F. AGASSANT, P. AVENAS and J. Ph. SERGENT, "La Mise en Forme des Matières Plastiques - Approche Thermomcanique", Technique et Documentation Lavoisier, Paris (1986).
23. P. E. ROUSE, *J. Chem. Phys.* **21** (1953) 1272.
24. B. H. ZIMM, *ibid.* **24** (1956) 269.
25. J. HEIJBOER, *Ann. New York Acad. Sci.* **279** (1976) 104.
26. R. F. BOYER, *Polymer* **17** (1976) 996.
27. R. KOHLRAUSCH, *Ann. Phys. Lpz* **12** (1847) 393.
28. L. C. E. STRUIK, "Physical Aging in Amorphous Polymers and Other Materials", Elsevier, Amsterdam (1978).
29. J. PEREZ, *J. Phys., Colloque C9* **44** (1983) 3.
30. E. POLAK, "Computationnal Methods in Optimization", Academic Press, New York (1971).
31. K. W. BRODLIE, in "The State of Art in Numerical Analysis" (edited by D. A. H. Jacobs) Academic Press, London (1977).
32. C. G'SELL and J. J. JONAS, *J. Mater. Sci.* **16** (1981) 1956.
33. E. H. LEE, T. G. ROGERS and T. C. WOO, *J. Amer. Ceram. Soc.* **48** (1985) 480.
34. R. DAVIAUD and G. FILLIATRE, "Introduction aux Matériaux Composites", Vol. I. C.N.R.S., Paris (1983).
35. S. W. TSAI and H. T. HAHN, "Introduction to Composite Materials", Technomic Publication, Westport (1980).
36. J. V. NOYES and B. H. JONES, Proceedings of the 9th AIAA/ASME Conference on "Structure, Dynamics and Material" (1968), Paper 68–336.
37. J. J. HERMANS, *Proc. Konikl. Neder. Akad. Westenschappen* **B70** (1967) 1.
38. W. AICHELE and M. DIEZ, *Kunstostoffe* **77** (1987) 168.
39. G. M. BARTENEV, *Zh. Tekhn. Fiz.* **19** (1949) 1423.
40. O. S. NARAYANASWAMY, *J. Amer. Ceram. Soc.* **52** (1969) 554.
41. E. H. LEE and T. G. ROGERS, *J. Appl. Mech.* **30** (1963) 127.

Received 26 November 1987
and accepted 29 April 1988